

Directed Transport of Confined Brownian Particles with Torque

Paul K. Radtke and Lutz Schimansky-Geier

Department of Physics, Humboldt-Universität zu Berlin, Newtonstr. 15, 12489 Berlin, Germany

We investigate the influence of an additional torque on the motion of Brownian particles confined in a channel geometry with varying width. The particles are driven by random fluctuations modeled by an Ornstein-Uhlenbeck process (OUP) with given correlation time τ_c . The latter causes persistent motion and is implemented as (i) thermal noise in equilibrium and as (ii) noisy propulsion in nonequilibrium. In the nonthermal process a directed transport emerges, its properties are studied in detail with respect to the correlation time, the torque and the channel geometry. Eventually, the transport mechanism is traced back to a persistent sliding of particles along the even boundaries in contrast to scattered motion at uneven or rough ones.

PACS numbers: 05.40.-a, 87.17.Jj

Introduction. Nowadays, ratchet models are employed to explain a wide range of transport phenomena, in biophysics as well as in artificial devices [1, 2]. Generally, the term ratchet refers to nonequilibrium phenomena that can arise provided one of the space-time symmetries that inhibits directed motion is broken [3]. This can be caused either explicitly by an asymmetric, periodic structure or by an unbiased, but asymmetric drive [4]. In our case, the symmetry breaking is realized by a nonvanishing mean torque together with the confining geometry.

The torque leads to a circular motion and an alteration of the diffusive properties [5]. Such motion appears in many real world phenomena. For example, it can be due to asymmetries in the propulsion of agents themselves as occurring in the chemotaxis of sperm cells [6–8] and nanorods [9, 10]. Also, a torque appears for Janus particles under laser irradiation [11] or due to an external magnetic field that is used to steer nanorods [12].

Furthermore, our particles are confined in an infinitely long channel with a periodically varying width, see Fig. 1. One channel boundary is introduced as a reflecting disk. Later on it will be interchanged by a reflecting triangle, thereby adding another symmetry breaking. Finally, we also consider a ‘rough’ lower wall where elastic scattering is modeled by equidistributed reflection angles, regardless of the angle of incidence.

Even though related studies of transport mechanisms possess some of the features, such as the channel layout in chaotic transport in Hamiltonian systems [13, 14], entropic particle transport [15] or for confined biological agents [8], its combination with a dissipative dynamics and a nonzero mean torque to realize directed transport is a novel feature. Hereby, the actual driving of the particles is performed by the noise, which delivers a constant energy supply.

Thermal Colored Noise. In our setting the particle has unit mass $m = 1$, position $\mathbf{r}(t) = (x(t), y(t))$ and velocity $\dot{\mathbf{r}}(t) = \mathbf{v}(t) = (v_x(t), v_y(t))$ at time t , that are driven by correlated noise $\boldsymbol{\epsilon}(t) = (\epsilon_x(t), \epsilon_y(t))$. Such noise is called colored, its memory causes a persistent motion. We choose an OUP to drive our particles, which is a common implementation for it represents the most

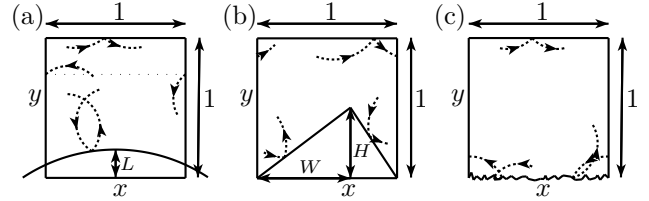


FIG. 1. Illustration of the channel geometry, a box of unit size whose left and right side are identified with each other, realizing periodic boundary conditions. At the top and bottom specular reflections take place. (a) Lower boundary formed by a disk of radius $R = 1.2$ that protrudes by $L = 0.2$ into the box. (b) Edged boundary parameterized by $H = 0.5$ and $W = 2/3$. (c) Flat lower boundary with equidistributed scattering angles due to a ‘rough’ surface.

natural continuous valued colored noise [16]. In equilibrium a fluctuation dissipation relation (FDR) relates the autocorrelation function of the noise and the friction function

$$\langle \epsilon_i(s) \epsilon_j(s+t) \rangle = \frac{\mathcal{D}_\xi}{\tau_c} e^{-|t|/\tau_c} \delta_{ij} = kT \gamma(|t|) \delta_{ij}, \quad (1)$$

with $i, j \in \{x, y\}$. Here the Einstein relation $\mathcal{D}_\xi = \gamma_0 kT$ (γ_0 – friction constant, k – Boltzmann constant, T – temperature) is used to relate the noise intensity \mathcal{D}_ξ to the heat bath from which the noise derives. Assuming that a FDR holds, we are forced to relinquish the Markov property by introducing a dissipative memory kernel $\gamma(|t-s|)$ to govern the friction. We then speak of a generalized Langevin equation [17, 18] for the velocity,

$$\dot{\mathbf{v}}(t) = - \int_0^t \gamma(t-s) \mathbf{v}(s) ds + \boldsymbol{\epsilon}(t) + \bar{\boldsymbol{\Omega}} \mathbf{v}(t). \quad (2)$$

The mean torque is realized by multiplication of \mathbf{v} with the rotation matrix $\bar{\boldsymbol{\Omega}}$, resulting in the force $\bar{\boldsymbol{\Omega}} \mathbf{v} = (\Omega v_y, -\Omega v_x)$.

Without confinement, the stationary Fokker-Planck equation corresponding to this dynamics is easily solved. We then find that the velocity is Maxwell-Boltzmann distributed. Numerically, we can confirm that this holds true in the channel geometry as well, both globally for

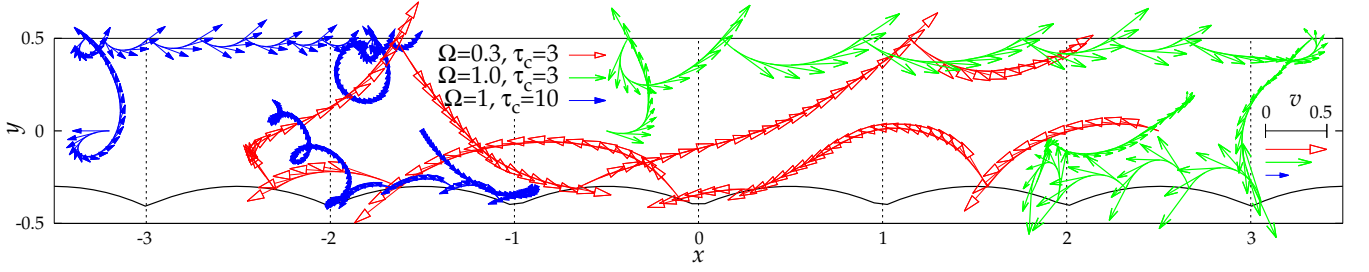


FIG. 2. (Color online) Trajectories of confined (cf. Fig. 1 (a)) particles exposed to nonthermal colored noise with several torques and correlation times at constant $\gamma_0 = 0.2$, $\mathcal{D}_\xi = 0.04$. The depicted time length is $t_l = 33$, the velocity is indicated by the arrows, between two consecutive arrows $\Delta t = 1/4$ has passed.

the entire channel and in the vicinity of the boundaries. Hence we have a symmetrical velocity distribution and no directed transport occurs.

The particles perform an undirected diffusive motion. As an estimate one can take the effective diffusion coefficient of this dynamics calculated for unbounded space, which reads [18]

$$D_{\text{eff}} = \mathcal{D}_\xi / (\gamma_0^2 + \Omega^2). \quad (3)$$

Apparently, it does not depend on the correlation time and coincides with the expression for particles driven by white noise.

Nonthermal Colored Noise. In the second case we consider noisy propulsion in nonequilibrium, hence no FDR holds [19]. Again equipped with an OUP-driving, our system is governed by the set of Langevin equations

$$\begin{aligned} \dot{\mathbf{r}}(t) &= \mathbf{v}(t), & \dot{\mathbf{v}}(t) &= -\gamma_0 \mathbf{v}(t) + \bar{\Omega} \mathbf{v}(t) + \boldsymbol{\epsilon}(t), \\ \dot{\boldsymbol{\epsilon}}(t) &= -\frac{1}{\tau_c} \boldsymbol{\epsilon}(t) + \frac{\sqrt{2\mathcal{D}_\xi}}{\tau_c} \boldsymbol{\xi}(t). \end{aligned} \quad (4)$$

Here $\boldsymbol{\xi}(t)$ denotes white Gaussian noise of zero mean with uncorrelated components, i.e. $\langle \xi_i(t) \rangle = 0$ and $\langle \xi_i(s) \xi_j(s+t) \rangle = \delta(t) \delta_{ij}$.

In this way, we have effectively realized the motion of an active particle, it underlies a permanent correlated supply of energy from the OUP-noise which it dissipates during the persistent and curved motion due to Stokes friction. The persistence of this motion expresses nonequilibrium. With $\tau_c \rightarrow 0$ white noise follows realizing again an equilibrium situation.

By taking the Fourier transforms of eq. (4), the spectrum of the velocity can be traced back to that of the noise

$$S_{v_i v_j}(\omega) = \frac{(\omega^2 + \gamma_0^2 + \Omega^2)}{(\gamma_0^2 + \Omega^2 - \omega^2)^2 + 4\omega^2 \gamma_0^2} S_{\epsilon_i \epsilon_j}(\omega). \quad (5)$$

With the Wiener-Khintchine theorem and the Lorentzian noise spectrum of the OUP $S_{\epsilon_i \epsilon_j}(\omega) = 2\mathcal{D}_\xi (1 + \tau_c^2 \omega^2)^{-1} \delta_{ij}$, which follows from the left-hand side of eq. (1), we obtain a rather lengthy expression for $\langle v(s)v(s+t) \rangle$. For $t = 0$ it simplifies to

$$\langle v_i v_j \rangle = \frac{\mathcal{D}_\xi}{\gamma_0} \frac{\gamma_0 \tau_c + 1}{(\gamma_0 \tau_c + 1)^2 + \Omega^2 \tau_c^2} \delta_{ij}. \quad (6)$$

Obviously, the torque, the friction, and the correlation time dampen the particles' mean squared velocity. For a vanishing mean torque the result without external force field [19] is reproduced.

We notice that the unconfined effective diffusion coefficient can be calculated from the Fourier transform of eq. (5) by integration over the time, which leads to the same result as for thermal colored noise (cf. eq. (3)).

Directed Transport in Confined Geometries.

Fig. 2 depicts some trajectories in the circular channel for the nonthermal dynamics given by eq. (4). Rising correlation times lead to a reduction of the total spatial displacements as do increasing mean torques, although less severely. With both influences acting on the particles together, another effect can be observed: The particles stay in the vicinity of the reflecting boundaries for a longer time and perform a curly hopping motion that changes to a narrow creeping for large τ_c [20]. Also, we notice that while the red trajectory (empty arrowheads) is largely unbiased, with bigger torques the particles travel a longer distance along the flat wall than along the curved wall.

The velocity distributions for the same situation are depicted in Fig. 3 [21]. While the velocity is Gaussian distributed for $\tau_c = 0$, it remains symmetrical on an unbounded plane or in the confined geometry without constant torque. In contrast, if all these influences act on the particles together, i.e. boundaries, finite correlation time and constant torque field, the velocity distribution loses its symmetry (green circles). For $\Omega = 1$, the v_x -distribution's left tail is lowered, while its right tail is raised. Thus, we have a net particle flux. Unlike for particles in equilibrium, the velocity distributions are narrowing with growing $|\Omega|$. Furthermore, we notice that the confinement particularly leads to a narrowing in $P(v_y)$, which now markedly differs from $P(v_x)$.

Let us now address the stationary particle fluxes J that pass in the x -direction through our channel. Herein, J is normalized with respect to the number of particles.

The numerical results for the net transport are shown in Fig. 4 as a function of the correlation time for several values of the mean torque. The flux J has a maximum at approximately $\tau_c \approx 2 - 3$ for all depicted Ω values. For vanishing correlation times, J converges to zero, which is consistent in view of the white noise case that follows

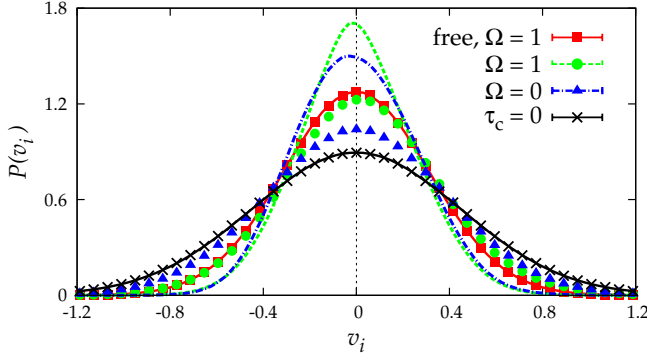


FIG. 3. (Color online) Velocity distribution (v_x – symbols, v_y – lines) for particles driven by nonthermal colored noise with $\tau_c = 1$, $\gamma_0 = 0.2$, $\mathcal{D}_\xi = 0.04$. Except for the red distribution (squares), particles are confined as in Fig. 1 (a). For $\tau_c = 0$, the same Gaussian distribution emerges regardless of Ω .

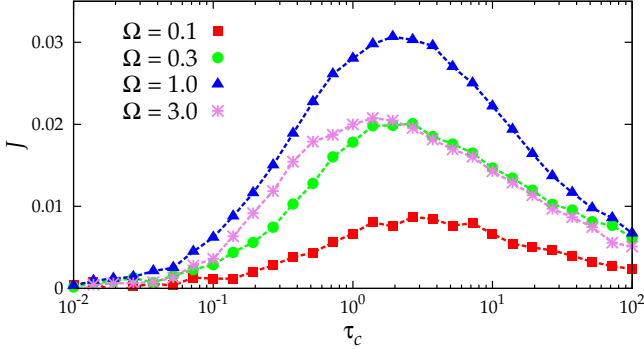


FIG. 4. (Color online) Net transport for particles driven by nonthermal colored noise for several mean torques at $\gamma_0 = 0.2$, $\mathcal{D}_\xi = 0.04$. The channel geometry is specified in Fig. 1 (a).

in this limit. There, the equilibrium condition forbids directed transport as the noise strength in eq. (4) vanishes. For large correlation times the net transport also converges to zero.

The effect of the mean torque is examined in further detail for several geometries in Fig. 5. Evidently, J vanishes for $\Omega = 0$ and also for strong torques regardless of the mean turning direction. The direction of the net transport changes with the orientation of Ω .

Given the emergence of a directed transport, we can justify its qualitative form, i.e. the asymptotics in τ_c and Ω as well as the occurrence of a maximum, with regard to the behavior of the speed. As implied by eq. (6) it vanishes both for large mean torques and correlation times. For transport to take place however, we need a torque to break the symmetry, and a nonzero correlation time for nonequilibrium. Hence we have no transport in either of the cases $\Omega \rightarrow 0$ or $\Omega \rightarrow \infty$ and $\tau_c \rightarrow 0$ or $\tau_c \rightarrow \infty$, leaving only a maximum value in between, which has to change its direction with the sign if the sign of the torque switches.

We now turn to the effects of the differing geometries in more depth. As we see in Fig. 5, the antisymmetrical behavior in Ω is conserved only as long as the lower bound-

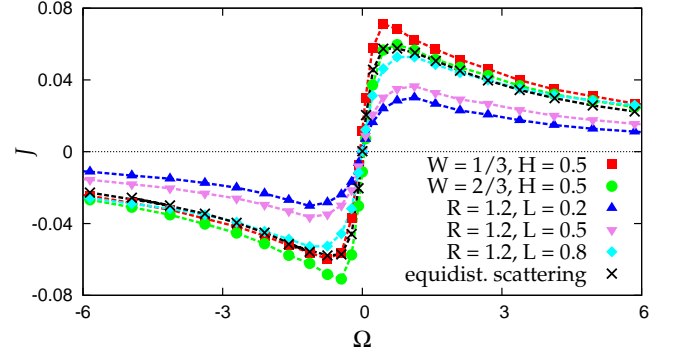


FIG. 5. (Color online) Net transport for various confining geometries (cf. Fig. 1). All curves are at $\gamma_0 = 0.2$, $\mathcal{D}_\xi = 0.04$ and $\tau_c = 3$.

ary keeps as left-right symmetry (cf. Fig. 1 (a,c)). Otherwise, as for the edged boundaries (cf. Fig. 1 (b)), the heights of the positive and negative peaks differ, whereas the direction of the current coincides for $W = 1/3$ and $W = 2/3$ (i.e. is independent of the orientation of the sawteeth). Also, the position of the maximum moves to slightly smaller Ω values for the edged surface compared to the disk.

If we narrow the channel by increasing the origin of the reflecting disk, the resulting transport curves also rise. However, their overall behavior remains; in particular the position of the maximum is barely altered and remains at $\Omega^{\max} \approx 1 - 1.5$. From this we conclude that the position of the Ω^{\max} cannot be traced to some resonant-like effect between the channel width and the cyclotron radius $R_c = v/\Omega$. Rather, the position of Ω^{\max} , as well as τ_c^{\max} , is a tradeoff between the necessary symmetry breaking and the reduction of the particles' speed.

Due to the unit scaling of the velocity, our net flux is identical to the mean velocity in the x -direction, $J = \langle v_x \rangle$. Other correlation ratchets [22, 23] display values for $\langle v_x \rangle$ in the same order of magnitude.

Elucidation of the Transport Mechanism. There are three possible types of trajectories in our channel: particles in the middle perform a more or less circular motion without net bias, whose regularity is enhanced by Ω and decreased by \mathcal{D}_ξ and γ_0 . Particles near the top eventually collide with the wall and are reflected. A counter clockwise mean turning rate then results in a forward motion and multiple further reflections. If we consider a particle that is driven to the wall by a noise pointing into that particular direction, the noise works largely as a drag force after reflection. It is still oriented in the same direction, whereas the particle has changed its own. As a result, the velocity normal to the boundary decreases (cf. Fig. 3). Once the noise orientation has changed (after about $\Delta t \approx \tau_c$), the particle is driven away from the boundary, although this may be counteracted by the particle's inertia together with the torque. Such situations are shown in Fig. 2. Clearly visible are the repeated reflections with ever decreasing radius and

speed at the top.

Without additional obstacle, particles near the bottom perform an antagonistic motion that cancels out the forward flux. The obstacle on the other hand modulates the reflection angles depending on the point of incidence. As seen in Fig. 2, the distance the particles have to travel until the next reflection varies depending on whether the surface tangential is increasing or decreasing. This constitutes a scattering effect that helps particles to escape from the vicinity of the boundary.

Hence the backward flux is hindered and a positive net transport emerges. In this picture, we can also explain the augmentation of J with the narrowing of the channel (cf. Fig. 5), for the particles cannot move as far without interaction with the boundaries. Thusly, the proportion of intermediate unbiased motion is reduced and the impact of the symmetry breaking is enhanced.

We confirm this rationale by considering a box with a flat but rough lower boundary, modeled by random equidistributed reflection angles (cf. Fig. 1 (c) and Fig. 5, black symbols). Obviously, this leads to a similar behavior of J .

Consequently, the flux is dominated by the sliding motion along the flat boundary and affected by the persistence, the torque and the noise driven velocity. In contrast, the geometry of the confinement and the shape of the lower boundary appear to be less important and influence the total value of J rather than its form. To evaluate qualitatively the dynamical dependence of the current, we expect that $J = J(\tau_c, \Omega, |\mathbf{v}|)$. It has to vanish if any of these three parameters vanishes, which favors a product of them. We can assume proportionality to the

velocity, which we approximate by $\sqrt{\langle \mathbf{v}\mathbf{v} \rangle}$. Then, the dependence from the torque is met by an additional factor $\sqrt{\Omega}$. The flux J rises linearly for small τ_c , in comparison to the numerical results this must be supplemented by an additional damping for large ones. Hence we propose $J \propto \text{sgn}(\Omega) \sqrt{|\Omega|} \langle \mathbf{v}\mathbf{v} \rangle \tau_c \exp(-\tau_c/4)$, which mimics the numerical results quite well. It yields a optimal torque at $|\Omega^{\max}| = \tau_c^{-1} + \gamma$, where the transport has a maximum of $J^{\max} \propto \tau_c \exp(-\tau_c/4)$. This behavior can also be seen in Fig. 4, where Ω^{\max} wanders to slightly smaller values with τ_c , and in the height of the corresponding peaks. It can be interpreted as a time scale merging between the period due to the torque, which is proportional to $1/\Omega$, and the two relaxation times τ_c and $\tau_{\text{inertia}} = 1/\gamma$ that characterize the persistence of the motion.

In conclusion, we have constructed a setup in which unbiased correlated noise is rectified in nonequilibrium and leads to the emergence of directed transport. To that end, we needed a nonzero mean torque and an asymmetric confining channel. We have given a qualitative explanation of the mechanism that leads to this symmetry breaking, namely the particle hopping along the boundaries disrupted by the scattering effect of the reflecting disk or triangle. Despite the general settings of the propulsion, particles and geometry, this investigation can help in the qualitative understanding and might be the starting point for more precise application oriented modeling of noisy active particles.

Acknowledgments. This paper was developed within the scope of the IRTG 1740 funded by the DFG. We acknowledge fruitful discussions with C. van den Broeck, T. Dittrich and B. Sonnenschein.

-
- [1] P. Hänggi and F. Marchesoni, *Rev. Mod. Phys.*, **81**, 387 (2009).
 - [2] P. Reimann, *Phys. Rep.*, **361**, 57 (2002), ISSN 0370-1573.
 - [3] S. Flach, O. Yevtushenko, and Y. Zolotaryuk, *Phys. Rev. Lett.*, **84**, 2358 (2000).
 - [4] I. Goychuk and P. Hänggi, *J. Phys. Chem. B*, **105**, 6642 (2001).
 - [5] C. Weber, P. K. Radtke, L. Schimansky-Geier, and P. Hänggi, *Phys. Rev. E*, **84**, 011132 (2011).
 - [6] B. M. Friedrich and F. Jülicher, *New J. Phys.*, **10**, 123025 (2008); *Phys. Rev. Lett.*, **103**, 68102 (2009), ISSN 1079-7114.
 - [7] B. M. Friedrich, I. Riedel-Kruse, J. Howard, and F. Jülicher, *J. Exp. Biol.*, **213**, 1226 (2010).
 - [8] S. Van Teeffelen and H. Löwen, *Phys. Rev. E*, **78**, 020101 (2008).
 - [9] A. Sen, M. Ibele, Y. Hong, and D. Velegol, *Faraday Discuss.*, **143**, 15 (2009).
 - [10] T. Mirkovic, N. Zacharia, G. Scholes, and G. Ozin, *Small*, **6**, 159 (2010).
 - [11] H. R. Jiang, N. Yoshinaga, and M. Sano, *Phys. Rev. Lett.*, **105**, 268302 (2010).
 - [12] T. Kline, W. Paxton, T. Mallouk, and A. Sen, *Angewandte Chemie*, **117**, 754 (2005).
 - [13] H. Schanz and M. Prusty, *J. Phys. A*, **38**, 10085 (2005); M. Prusty and H. Schanz, *Phys. Rev. Lett.*, **96**, 130601 (2006), ISSN 1079-7114.
 - [14] W. Acevedo and T. Dittrich, *Prog. Theor. Phys. Supp.*, **150**, 313 (2003).
 - [15] S. Martens, G. Schmid, L. Schimansky-Geier, and P. Hänggi, *Phys. Rev. E*, **83**, 051135 (2011).
 - [16] P. Hänggi and P. Jung, *Adv. Chem. Phys.*, **89**, 239 (1995).
 - [17] H. Mori, *Prog. Theor. Phys.*, **34**, 399 (1965).
 - [18] F. N. C. Paraan, M. P. Solon, and J. P. Esguerra, *Phys. Rev. E*, **77**, 022101 (2008).
 - [19] L. H'walisz, P. Jung, P. Hänggi, P. Talkner, and L. Schimansky-Geier, *Z. Phys. B*, **77**, 471 (1989).
 - [20] A sliding along the channel walls has also been studied in [8] and observed experimentally, see P. Dhar, T. Fischer, Y. Wang, T. Mallouk, W. Paxton, and A. Sen, *Nano Lett.*, **6**, 66 (2006).
 - [21] Errorbars are of symbol size and hence omitted.
 - [22] R. Bartussek, P. Reimann, and P. Hänggi, *Phys. Rev. Lett.*, **76**, 1166 (1996).
 - [23] B. Lindner, L. Schimansky-Geier, P. Reimann, P. Hänggi, and M. Nagaoka, *Phys. Rev. E*, **59**, 1417 (1999).